RP14

Integrated Numerical and Laboratory Rock Physics Applied to Seismic Characterization of Reservoir Rocks

E.H. Saenger* (ETH Zurich & Spectraseis AG), M. Frehner (ETH Zurich), C. Madonna (ETH Zurich), N. Tisato (ETH Zurich), M. Kuteynikova (ETH Zurich), N. Riahi (ETH Zurich), P. Sala (University of Bern) & B. Quintal (ETH Zurich)

SUMMARY

Identifying and understanding the physical processes taking place in a reservoir rock is an important step towards a more detailed and accurate characterization of a subsurface hydrocarbon reservoir from a seismic data set, and is the subject of our article. We show that the integration of laboratory studies with numerical modeling is a powerful tool to achieve an unbiased comprehension of the physical processes at different scales. Such integration is demonstrated in this article using examples of two current challenges in rock physics: (1) understanding the influence of the rock microstructure on effective elastic properties; (2) identifying the dominant physical mechanism responsible for intrinsic attenuation in saturated rocks at seismic frequencies. In the first example, we show how the coupling between laboratory and numerical methods help provide a better understanding of the effect of the rock microstructure on the effective P-wave velocity. Additionally, this procedure enabled the numerical computations to yield an accurate prediction of the P-wave velocity with confining pressure. In the second example, we show that laboratory or numerical studies alone can lead to misconception or misinterpretation of the obtained results. A persistent combination of laboratory and numerical methods is essential for a successful rock physics research.

Introduction

A good understanding of the effect of rock and pore fluid properties on seismic waves is necessary for the characterization of a subsurface hydrocarbon reservoir from a seismic data set. Punctual information about the rock and fluids in the reservoir can be obtained, for example, through well logging and laboratory tests with samples cored from the wellbore. Together with seismic data, this information can be extrapolated for the entire dimension of the reservoir providing quantitative estimates for production. This information can be also extrapolated in time for monitoring the spatial redistribution of fluids during production. Making more accurate such space and time predictions from seismic data is the main goal of rock physics. For that, identifying and understanding the physical processes taking place in a reservoir rock is an important step and the subject of our article. We show that the integration of laboratory studies with numerical modeling is a powerful tool to achieve an unbiased comprehension of the physical processes at different scales. In laboratory experiments it is very difficult, or even impossible, to control all the physical processes. However, in numerical simulations all physical parameters can be controlled exactly, and it is even possible to study different physical processes separately from each other, which otherwise coexist in nature or in the laboratory. The physical insight resulting from such numerical studies helps understand and better interpret results from laboratory experiments. This knowledge-feedback between laboratory and numerical rock physics is demonstrated in this article on examples of two current challenges in rock physics: (1) understanding the influence of the rock microstructure on effective elastic properties; (2) identifying the dominant physical mechanism responsible for intrinsic attenuation in saturated rocks at seismic frequencies. Both challenges are subject to ongoing research conducted in The Rock Physics Network at ETH Zurich and the studies presented in this article are a snapshot of work in progress.

Effect of the rock microstructure on effective elastic properties

X-ray micro-computed tomography (micro-CT) allows generating 3D digital models of real rocks (insets in Figure 1). Numerical modeling using such digital rock models combined with laboratory measurements can be used to predict properties of a reservoir rock. For example, simulating fluid flow through digital rock models yields a permeability estimate which is comparable with laboratory data (e.g., Knackstedt et al., 2009). The resolution of the micro-CT image is sufficient in this case because fluid predominantly flows through larger pores. However, mechanical properties, such as the effective elastic moduli, strongly depend on the grain contacts which might not be resolved by the micro-CT technique. In the following, laboratory experiments are coupled with numerical simulations to provide an understanding of the effect of the unresolved rock microstructure on the P-wave velocity.

a) Laboratory experiments

P-wave velocity, V_P, was measured at 3 MHz on a dry sample of Berea Sandstone (25.4 mm diameter, 40 mm length) at confining pressures, P_c, up to 200 MPa at room temperature. The resulting curve (open circles and solid line in Figure 1a) describes a non-linear increase of V_P with P_c up to 50 MPa, followed by a linear trend for higher values of P_c.

b) Numerical experiments

X-ray micro-CT imaging was performed on a core plug (6 mm diameter, 20 mm length) of the sample used in laboratory. The system consists of a SkyScan 1172 high-resolution desktop scanner providing a pixel size of 3.14 μm. A standard segmentation technique divides the raw data into three phases: quartz (main matrix), ankerite, and empty pores. The segmented micro-CT data provides a 3D digital model of the rock (right inset in Figure 1a). To calculate V_P we use the finite-difference method to propagate a plane P-wave with a central frequency of 3 MHz through the 3D digital rock model (Saenger et al., 2011). The

elastic moduli used for [quartz, ankerite] are K = [38, 73] GPa, G = [44, 32] GPa, and M = K+4G/3, where K, G, and M are, respectively, the bulk, the shear and the P-wave moduli. The pores were treated as vacuum. The result is shown in Figure 1a as a star.

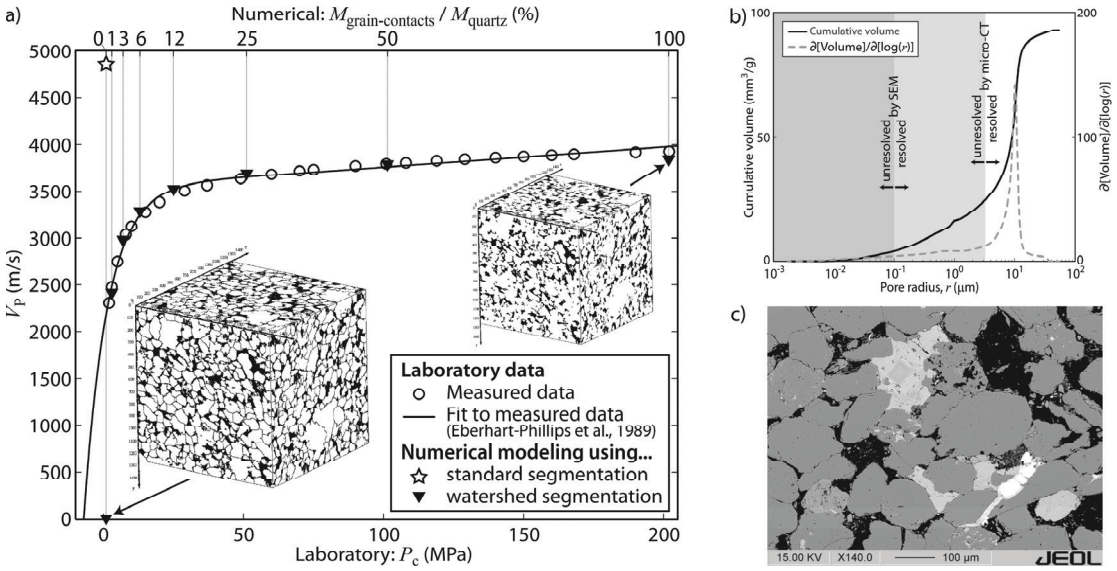

Figure 1. (a) Laboratory and numerical results for the P-wave velocity, V_P, at 3 MHz as a function of confining pressure, P_c, in a Berea Sandstone sample. (b) Mercury porosimetry measurements. (c) Scanning Electron Microscopy (SEM) image.

c) Integrated interpretation of laboratory and numerical results

In Figure 1a, the numerically calculated value of V_P is higher than all laboratory measurements, observation already reported by Knackstedt et al. (2009). In addition, it is not clear to which confining pressure such value corresponds (arbitrarily plotted at P_c = 0). A more detailed characterization of the rock microstructure reveals the cause of this discrepancy. Mercury intrusion porosimetry (Figure 1b) shows that 25% of the pore volume is below the resolution limit of the micro-CT imaging, and scanning electron microscopy (SEM) (Figure 1c) reveals that grain contacts and microcracks within grains remain unresolved in the micro-CT digital rock model (right inset in Figure 1a). We assume that the difference between numerical and laboratory results is mainly due to these unresolved microstructures.

To improve the digital rock model we apply watershed segmentation, which is a grain contact reconstruction method to locate grain contacts that are below the resolution of the micro-CT data (Arns et al., 2007). The grain contacts represent an additional phase in the digital rock model. In subsequent numerical simulations, an effective P-wave modulus, $M_{contacts}$, with values ranging from 0% to 100% of the P-wave modulus of quartz, M_{quartz}, is assigned to the grain contacts (assumed to be weaker than the quartz grains). We obtain the P-wave velocity as a function of $M_{contacts}/M_{quartz}$ (triangles as a function of upper abscissa in Figure 1a). If $M_{contacts}$ = 0 (left inset in Figure 1a), the grain contact phase represents a vacuum and V_P = 0. If $M_{contacts}$ = M_{quartz} (right inset in Figure 1a), the grain contact phase is effectively inexistent (as in the standard segmentation). Because the numerical results ($V_{P,num}$ versus $M_{contacts}/M_{quartz}$) show a similar trend as the laboratory measurements ($V_{P,lab}$ versus P_c), a linear data mapping between the two data sets can be done. The resulting pressure-dependent velocity ($V_{P,num}$ versus P_c) is shown as triangles as a function of lower abscissa in Figure 1a. The numerical method systematically overestimates the value of V_P, compared to the laboratory data, because of microstructures not detected with the watershed segmentation. However, a calibration with laboratory data enables the numerical approach to yield not only an accurate prediction of the velocity with pressure, but also an estimate of the effect of grain contacts.

Physical mechanism for attenuation at seismic frequencies

Attenuation of seismic waves in partially saturated porous rocks is of great interest because hydrocarbon reservoirs frequently exhibit high P-wave attenuation at seismic frequencies. When the dominant physical mechanisms for attenuation are identified, estimates of attenuation can improve interpretation of seismic data and information about the fluid may be inferred. In the following, we compare laboratory measurements of attenuation in a partially saturated rock sample in the low seismic frequency range, with results from numerical modeling for attenuation caused by the physical mechanism of wave-induced fluid flow using an idealized version of the same sample. The comparison of laboratory and numerical results is a way to verify or falsify the dominance of a particular physical mechanism for attenuation.

a) Laboratory experiments

We use the Broad Band Attenuation Vessel (BBAV; Tisato et al., 2011) to measure intrinsic bulk attenuation in a partially saturated rock sample (25 cm height, 7.6 cm diameter) by performing sub-resonance tests at frequencies ranging from 0.1 to 100 Hz. Calibration of the BBAV was successfully performed with aluminum and plexiglas. We measured attenuation in a sample of Berea Sandstone with a permeability of 600 mD, a porosity of 20%, and bulk and shear moduli of the dry frame of 7 GPa and 4.2 GPa, respectively. The measurements were performed at room pressure and temperature, even though confining pressures up to 25 MPa are achievable by the BBAV. The sample was sealed, and partially saturated with 60% water, 40% air. Figure 2a shows the measured quality factor, Q, as a function of frequency as dots and open circles. Attenuation is given by $1/Q$. To achieve the 60% partial water saturation, two saturation criteria were used. In one case, the water saturation in the sample was increased from 0% to 60%. In the other case, the water saturation was reduced from 90% to 60%. The two curves for Q exhibit a slight shift, particularly at higher frequencies. Because the same sample was used in both experiments, we deduce that the difference between the two curves is caused by different spatial distributions of water and air in the sample.

b) Numerical experiments

We numerically model attenuation caused only by wave-induced fluid flow due to patchy saturation at the mesoscopic scale (White, 1975). This mechanism is generally assumed to dominate attenuation at seismic frequencies. In a patchy saturated medium, a seismic wave causes pore-pressure differences between the patches fully saturated with one fluid and the surrounding medium fully saturated with another fluid. These pore-pressure differences are due to the different compressibilities of the two fluids. To calculate attenuation due to wave-induced fluid flow, we numerically perform quasi-static creep tests solving Biot's equations, as described by Quintal et al. (2011). The 3D numerical poroelastic sample has the same dimensions as the sample used in the laboratory. The properties of the solid frame are the same everywhere, and the same as the bulk properties of the laboratory sample. To simulate the partial saturation, three equally spaced spherical heterogeneities in fluid-saturation are aligned at the center of the numerical sample (Figure 2b). Two scenarios were chosen: air saturated patches and water saturated surrounding rock; and water saturated patches and air saturated surrounding rock. The radius of the three spherical heterogeneities is chosen such that a water saturation of 60% is achieved. We perform the numerical quasi-static tests using the finite-element software COMSOL Multiphysics. The results for Q (Figure 2a) almost perfectly coincide for the two scenarios. At higher frequencies, around the transition frequency, f_{tr}, the two curves slightly diverge.

c) Integrated interpretation of laboratory and numerical results

The numerical results for Q disagree with the laboratory results (Figure 2a). The values of Q are much greater than the values measured in laboratory. Also, the slopes of the curves for Q

are different in both cases. For the laboratory data the slope is around –0.25 in double-logarithmic representation, while for the numerical data the slope is –1, which is theoretically predicted for a periodic distribution of patches, and also for a random distribution in a finite medium. Because in the numerical simulations patchy saturation is the only cause of attenuation, the fundamental difference in slope leads to the conclusion that this is not the sole cause of attenuation in the laboratory measurements. It is possible that wave-induced fluid flow is still a dominant physical mechanism for attenuation, but the model consisting of three spherical patches of saturation may be a too rough idealization. It may also be an over-simplification to consider the solid frame homogeneous. Additionally, other attenuation mechanisms (e.g., squirt flow) must be investigated in future numerical studies.

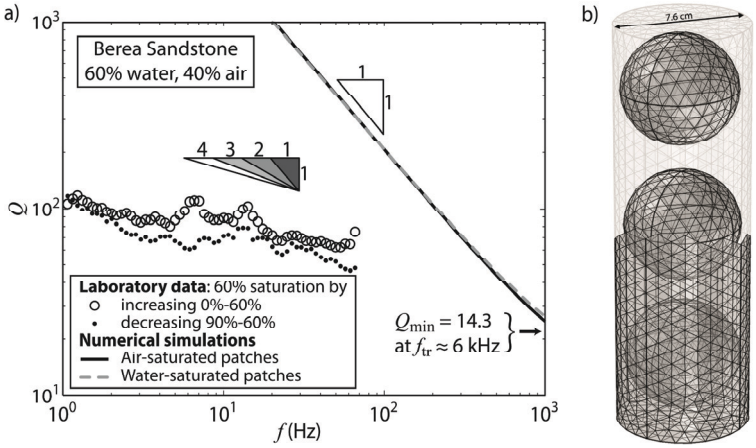

Figure 2. (a) Laboratory and numerical results for the quality factor, Q, as a function of frequency on a Berea Sandstone sample saturated with 60% water and 40% air. (b) 3D numerical sample with a tetrahedral finite-element mesh used for the numerical simulations.

Conclusions

We presented two ongoing research projects in the field of rock physics, where we integrate laboratory and numerical methods to better understand the relevant physical processes. Based on our experience, we can state that laboratory or numerical studies alone can lead to misconception or misinterpretation of the obtained results.

Acknowledgements

This work is supported by the Low Frequency Seismic Partnership (LFSP), Spectraseis, the Swiss Commission for Technology and Innovation (CTI), and the German Research Foundation (DFG).

References

Arns, C.H., Madadi, M., Sheppard, A.P. and Knackstedt, M.A. [2007] Linear elastic properties of granular rocks derived from X-ray-CT images. *SEG Expanded Abstracts*.

Knackstedt, M.A., Latham, S., Madadi, M., Sheppard, A., Varslot, T. and Arns, C. [2009] Digital rock physics: 3D imaging of core material and correlations to acoustic and flow properties. *The Leading Edge*, **28**, 28–33.

Quintal, B., Steeb, H., Frehner, M. and Schmalholz, S.M. [2011] Quasi-static finite element modeling of seismic attenuation and dispersion due to wave-induced fluid flow in poroelastic media. *Journal of Geophysical Research*, **116**, B01201.

Saenger, E.H., Enzmann, F., Keehm, Y. and Steeb, H. [2011] Digital rock physics: Effect of fluid viscosity on effective elastic properties. *Journal of Applied Geophysics*, **74**, 236–241.

Tisato, N., Madonna, C., Artman, B. and Saenger, E.H. [2011] Low frequency measurements of seismic wave attenuation in Berea sandstone. *SEG Expanded Abstracts.*

White, J.E. [1975] Computed seismic speeds and attenuation in rocks with partial gas saturation. *Geophysics*, **40**, 224–232.